

A Robust Tracking Controller for Electrically Driven Robot Manipulators: Stability Analysis and Experiment

Mohamadreza Homayounzade¹ Mehdi Keshmiri¹ Mostafa Ghobadi²

¹Department of Mechanical Engineering, Isfahan University of Technology (IUT), Isfahan, Iran

²Department of Mechanical Engineering, University at Buffalo SUNY, New York, USA

Abstract: In this paper, a robust controller for electrically driven robotic systems is developed. The controller is designed in a backstepping manner. The main features of the controller are: 1) Control strategy is developed at the voltage level and can deal with both mechanical and electrical uncertainties. 2) The proposed control law removes the restriction of previous robust methods on the upper bound of system uncertainties. 3) It also benefits from global asymptotic stability in the Lyapunov sense. It is worth to mention that the proposed controller can be utilized for constrained and nonconstrained robotic systems. The effectiveness of the proposed controller is verified by simulations for a two link robot manipulator and a four-bar linkage. In addition to simulation results, experimental results on a two link serial manipulator are included to demonstrate the performance of the proposed controller in tracking a given trajectory.

Keywords: Electrically driven robots, Lyapunov stability, parametric uncertainty, robust control, uncertain actuator dynamics.

1 Introduction

System uncertainties arising from errors in system modeling, variation of system parameters and unmodelled physical phenomena such as unstructured friction, are inevitable and produce an extra difficulty in the process of controller design^[1, 2].

Various control techniques have been evolved to mitigate the effects of uncertainties for decades and have recently reattracted notable attentions from both industry and academic investigation. Among these methods, robust and adaptive methods provide appealing and efficient approaches to handle the control analysis and synthesis of uncertain and ill-defined complex nonlinear systems.

In the adaptive approach, the controller learns the parameter uncertainties and gets tuned with the parameter variations. Hence adaptive method can be used for a wide range of system uncertainties. Since the controller parameters should be updated with the uncertainty variations, this method is a time consuming approach^[2].

In the past decades, robust control of uncertain nonlinear dynamics has undergone rapid developments and there have been developed a lot of robust control methods such as linear-quadratic-Gaussian (LQG), loop transfer recovery (LTR), H_∞ control, sliding mode control and etc. In contrast to adaptive controllers, a robust controller has a fixed structure which yields an acceptable performance for a restricted range of uncertainties. A robust controller does not need the exact functional nature of the model^[3], however it requires some knowledge about bounding functions on the

largest possible size of the uncertainties^[1].

A systematic framework for tackling a robust output regulation problem for general uncertain nonlinear systems was given in [4–6]. It was evolved from the proposed approach in [1] and deals with a local robust output regulation problem through an output feedback control. In [7], a constant bound for parametric uncertainties is assumed. Different uncertainty bounds have been considered for designing robust robot controllers^[8–16]. Unstructured uncertainty bound has been usually considered as a constant^[8, 9] or as a function of state variables^[10–16].

Actuator dynamics contemplate as a significant component of the entire robot dynamics, particularly in the cases of high-velocity maneuver and highly varying loads^[17]. Contemplating the actuators into the dynamic equations engenders the system dynamics to be described by a set of third-order differential equations and complicates the controller design and its stability analysis^[18]. Control of rigid robots including actuator dynamics is still an open forum in the literature^[19–25].

The main subject of this paper is to deal with trajectory tracking of electrically driven robotic systems considering uncertainties in both mechanical and electrical subsystems. The overall controller is designed through a backstepping approach.

The main contribution of this paper can be addressed as:

1) Relaxing the restrictive assumption made on the largest possible size of the system uncertainties. In [16], we have developed a robust controller for robotic systems. The proposed method like many conventional methods is suffering from the restricted range of applications due to the bound made on the system uncertainties (especially the inertia matrix). This restriction will be removed through

Regular paper
Manuscript received February 4, 2013; accepted March 13, 2014
Recommended by Associate Editor Guo-Ping Liu
©Institute of Automation, Chinese Academy of Science and Springer-Verlag Berlin Heidelberg 2015

the deployment of the new method.

2) The presented method improves the performance of the system in tracking any given desired trajectories such that it results in global asymptotic stability of the system.

3) In the majority of the previous researches, the actuator dynamics is neglected, while in this study actuators dynamics as well as their uncertainties are taken into account in the development of the controller.

The remainder of this paper is organized as follows. In Section 2, dynamical model of electrically driven robots and its properties are presented. In Section 3, the controller is designed. Section 4 analyzes the stability of the proposed model. In Section 5, the proposed controller will be extended to constrained robotic systems. The numerical and experimental results for two different case studies; a two link serial manipulator and a four-bar linkage, are presented in Section 6. Section 7 concludes the analysis.

2 Dynamic modeling of robotic systems

In this section, initially we present the governing dynamic equations of an n -link manipulator. Then two useful properties related to these equations are summarized.

2.1 Equations of motion

Based on the Euler-Lagrange formulation, the motion equations of an n -link rigid manipulator can be represented as

$$M'(q)\ddot{q} + C'(q, \dot{q})\dot{q} + g'(q) + J_f^T \tau_d + f'(\dot{q}) = \tau \quad (1)$$

where $q \in \mathbf{R}^n$ is the generalized coordinates (joint positions), $\tau \in \mathbf{R}^n$ is the actuating torques vector, $M'(q) \in \mathbf{R}^{n \times n}$ is the inertia matrix, $C'(q, \dot{q}) \in \mathbf{R}^n$ represents the centripetal and coriolis torques, $g'(q) \in \mathbf{R}^n$ is the vector of gravitational torques, $f'(\dot{q}) \in \mathbf{R}^n$ represents friction terms, $\tau_d \in \mathbf{R}^n$ represents unknown bounded constant disturbance vector represented in the Cartesian workspace and $J_f \in \mathbf{R}^{n \times n}$ is the Jacobian matrix calculated by

$$J_f' = \frac{\partial r_f}{\partial q} \quad (2)$$

where r_f is the foot point of τ_d , and it is assumed to be uncertain.

The brushed direct current (BDC) motors dynamics can be modeled as

$$L_m \dot{I} + R_m I + K_{em} \dot{q} = v \quad (3)$$

where $I \in \mathbf{R}^n$ is the vector of the armatures current, $v \in \mathbf{R}^n$ is the vector of armatures voltage, $L_m \in \mathbf{R}^{n \times n}$ is the actuators inductance matrix, $R_m \in \mathbf{R}^{n \times n}$ is the actuators resistance matrix and $K_{em} \in \mathbf{R}^{n \times n}$ is the motors back emf coefficient matrix.

The correlation between motors current and torque is defined by

$$\tau = K_{Tm} I \quad (4)$$

where $K_{Tm} \in \mathbf{R}^{n \times n}$ is the motors electromechanical coefficients. Note that R_m, L_m, K_{em} and K_{Tm} are all diagonal and positive definite constant matrices.

Rewriting (1) with a new notation, one obtains

$$M(q)\ddot{q} + C(q, \dot{q})\dot{q} + g(q) + J_f^T \tau_d + f(\dot{q}) = I \quad (5)$$

where

$$\begin{aligned} M(q) &= K_{Tm}^{-1} M'(q) \\ C(q, \dot{q}) &= K_{Tm}^{-1} C'(q, \dot{q}) \\ g(q) &= K_{Tm}^{-1} g'(q), \quad f(\dot{q}) = K_{Tm}^{-1} f'(\dot{q}) \\ J_f &= J_f'(q) K_{Tm}^{-T}. \end{aligned} \quad (6)$$

Definition 1. For an arbitrary positive definite or negative definite symmetric matrix such as B , throughout this paper, by B_m and B_M the authors mean the minimum and maximum eigenvalues of that matrix. Hence, for any arbitrary vector x , we can state,

$$B_m \|x\|^2 \leq x^T B x \leq B_M \|x\|^2. \quad (7)$$

Note that $\|\cdot\|$ represents the 2 induced norm for matrices and Euclidean norm for vectors.

2.2 Properties of the equation of motion

Structure of the equations of motion expressed by (5) benefits from the following properties which will be used in the development of the control law.

Property 1. The inertia matrix $M(q)$ is known to be positive definite and symmetric.

Property 2. A suitable definition of $C(q, \dot{q})$ makes the matrix $\frac{1}{2}\dot{M} - C$ skew symmetric. In particular, the elements of $C(q, \dot{q})$ may be defined as

$$C_{ij}(q, \dot{q}) = \frac{1}{2} \left[\dot{q}^T \frac{\partial M_{ij}}{\partial q} + \sum_{k=1}^n \left(\frac{\partial M_{ik}}{\partial q_j} - \frac{\partial M_{jk}}{\partial q_i} \right) \dot{q}_k \right]. \quad (8)$$

Therefore (9) holds for any arbitrary vector $x \in \mathbf{R}^n$:

$$x^T \left[\frac{1}{2}\dot{M} - C(q, \dot{q}) \right] x = 0. \quad (9)$$

3 Controller design

Here initially the control law is proposed, and then it is substituted into the robot dynamic equation represented by (5) in order to obtain the final closed-loop error dynamics. This closed loop dynamics is then used in the Lyapunov analysis to show that this control law is appropriate to push the robotic system to track the desired trajectory.

3.1 Error dynamics

Introducing the desired joint positions and velocities by q_d and \dot{q}_d , and defining the modified error by

$$r = \Lambda e + \dot{e} \quad (10)$$

where $e = q - q_d$, $\dot{e} = \dot{q} - \dot{q}_d$ and $\Lambda = \text{diag} \{ \lambda_1, \dots, \lambda_n \}$, $\lambda_i > 0$. Equation (5) can be written

as

$$M \dot{r} = M(\Lambda \dot{e} - \ddot{q}_d) - C(q, \dot{q})(r - \Lambda e + \dot{q}_d) - g(q) - f(\dot{q}) - J_f^T \tau_d + I. \tag{11}$$

Since the robot equation is linear in parameters^[26], we can define the right side of (11) in the regression form as

$$Y_1(q, \dot{q}, t) \Phi_1 = M(\Lambda \dot{e} - \ddot{q}_d) - g(q) - f(\dot{q}) - C(q, \dot{q})(-\Lambda e + \dot{q}_d) - J_f^T \tau_d \tag{12}$$

where $Y_1(\cdot) \in \mathbf{R}^{n \times m}$ is the robot regressor matrix, $\Phi_1 \in \mathbf{R}^m$ represents uncertain mechanical parameters, is a constant vector, and m is the number of uncertain parameters.

Hence, (11) can be written as

$$M \dot{r} = Y_1(q, \dot{q}, t) \Phi_1 - C(q, \dot{q}) r + I. \tag{13}$$

3.2 Trajectory tracking control

A backstepping-like approach is used to design the controller for the system modeled by (5).

In the first step using the mechanical subsystem dynamics, a desired current signal I_d is calculated such that the trajectory tracking control is performed. Then in the second step, in order to enforce I tracks its desired values, I_d , the required voltage input, is determined using the electrical subsystem dynamics.

Let us define the desired current calculated by

$$I_d = -K_v r - Y_1(\cdot) \bar{\Phi}_1 + u_1 \tag{14}$$

where $K_v \in \mathbf{R}^{n \times n}$ is a positive definite symmetric gain matrix, $\bar{\Phi}_1$ represents the nominal values of the uncertain parameters, and u_1 is defined by

$$u_1 = -\frac{\rho_1^2 r}{\rho_1 \|r\| + \varepsilon^2}. \tag{15}$$

Since Φ_1 and $\bar{\Phi}_1$ are bounded constant vectors, hence we can assume that $\|\tilde{\Phi}_1\| \leq \alpha_1$, where $\tilde{\Phi}_1 = \Phi_1 - \bar{\Phi}_1$ and no restriction exists on the magnitude of α_1 . In (14), the term $-Y_1(\cdot) \bar{\Phi}_1$ represents the nonlinearity of robot (but calculated by nominal magnitudes of parameters) and the term $-K_v r + u_1$ is used to relieve the mismatch resulted from calculating the nonlinearities of robot with the nominal magnitude of uncertainties.

Now let us introduce ρ_1 and ε through the following equations:

$$\rho_1 = \alpha_1 \|Y_1(\cdot)\| \tag{16}$$

$$\dot{\varepsilon} = -K_\varepsilon \varepsilon. \tag{17}$$

where K_ε is a positive constant. Clearly ε is a continuously decaying positive function once $\varepsilon(0) > 0$.

Therefore, from the above equations, it can be concluded that

$$\|\dot{I}_d\| \leq \chi(\|e\|, \|\dot{e}\|, \|\ddot{e}\|, \|\ddot{q}_d\|). \tag{18}$$

where χ is a bounded function for bounded variables. Equation (18) implies that if the system tracking errors be bounded, an upper bound can be considered for the first derivative of the desired current as

$$\|\dot{I}_d\| \leq \alpha_3. \tag{19}$$

If we define the desired current tracking error by

$$\eta = I - I_d \tag{20}$$

and substitute $I = I_d + \eta$ in (13), we obtain

$$M \dot{r} = Y_1(\cdot) \tilde{\Phi}_1 - C(q, \dot{q}) r - K_v r + u_1 + \eta. \tag{21}$$

Hence, the electrical dynamics represented by (3) can be written in terms of the current error:

$$L_m \dot{\eta} = -R_m \eta - K_{em} \dot{q} - L_m \dot{I}_d - R_m I_d + v. \tag{22}$$

Similar to the mechanical subsystem, we introduce

$$Y_2(q, \dot{q}, \eta, t) \Phi_2 = -R_m \eta - K_{em} \dot{q} - R_m I_d \tag{23}$$

where $Y_2(\cdot) \in \mathbf{R}^{n \times p}$ is the electrical regressor matrix, $\Phi_2 \in \mathbf{R}^p$ is the vector of uncertain electrical parameters, and p represents the number of these parameters. Therefore (22) can be written as

$$L_m \dot{\eta} = Y_2(\cdot) \Phi_2 - L_m \dot{I}_d + v. \tag{24}$$

3.3 Desired current control

The second step in the controller design is introducing a control law for the input voltage such that the motor current tracks the calculated desired current. Let us introduce the following control law for the motor voltage

$$v = -Y_2(\cdot) \bar{\Phi}_2 - r + u_2 \tag{25}$$

where u_2 is similarly given by

$$u_2 = -\frac{\rho_2^2 \eta}{\rho_2 \|\eta\| + \mu^2}. \tag{26}$$

Similar to $\tilde{\Phi}_1$, it can be assumed that $\|\tilde{\Phi}_2\| \leq \alpha_2$ where $\tilde{\Phi}_2 = \Phi_2 - \bar{\Phi}_2$ and no restriction exists on the magnitude of α_2 .

In the above equation, ρ_2 is defined by

$$\rho_2 = \alpha_2 \|Y_2(\cdot)\| + l \alpha_3 \tag{27}$$

where l is a constant greater than the maximum eigenvalue of matrix L and again similar to ε , μ is an augmented state with the following dynamics as

$$\dot{\mu} = -K_\mu \mu. \tag{28}$$

μ is also a continuously decaying positive function once $\mu(0)$ and K_μ are positive constants.

Substituting (25) and (26) in (24), it can be deduced that

$$L_m \dot{\eta} = -L_m \dot{I}_d + Y_2(\cdot) \tilde{\Phi}_2 - \frac{\rho_2^2 \eta}{\rho_2 \|\eta\| + \mu^2} - r. \tag{29}$$

4 Stability analysis

Stability and performance of the whole control system in the trajectory tracking is analyzed by the following theorem. The Theorem 1 is developed based on the Lyapunov arguments where a positive definite Lyapunov function is shown to have a negative definite time derivative starting from a bounded initial state vector $\gamma = [e^T, \dot{e}^T]^T$.

Theorem 1. The input control voltage calculated by (25) results in semi-globally asymptotic stability of position and velocity tracking error, i.e.,

$$\lim_{t \rightarrow \infty} e = 0, \quad \lim_{t \rightarrow \infty} \dot{e} = 0 \tag{30}$$

provided that the desired trajectory tracking and the initial system errors γ being bounded.

Proof. Consider a so called positive definite Lyapunov function defined by

$$V(E) = \frac{1}{2} E^T P E \tag{31}$$

where $E = [r^T, \eta^T, \varepsilon, \mu]^T$ is the augmented state vector and

$$P = \text{diag} \{ M, L_m, K_\varepsilon^{-1}, K_\mu^{-1} \}. \tag{32}$$

Differentiating (31) with respect to time, we obtain

$$\dot{V} = r^T M \dot{r} + \eta^T L_m \dot{\eta} + \frac{1}{2} r^T \dot{M} r - \varepsilon^2 - \mu^2. \tag{33}$$

Substituting (21) and (24), it can be concluded that

$$\begin{aligned} \dot{V} = & r^T \left[Y(\cdot) \tilde{\Phi}_1 - K_v r - \frac{\rho_1^2 r}{\rho_1 \|r\| + \varepsilon^2} \right] + \\ & r^T \left[\frac{1}{2} \dot{M} - C(q, \dot{q}) \right] r + \eta^T \left[-L_m \dot{I}_d + Y_2(\cdot) \tilde{\Phi}_2 - \right. \\ & \left. \frac{\rho_2^2 \eta}{\rho_2 \|\eta\| + \mu^2} \right] - \varepsilon^2 - \mu^2. \end{aligned} \tag{34}$$

Utilizing Property 2 and considering (7) and the facts that for any arbitrary vectors such as a and b , we have $a^T b \leq \|a\| \|b\|$ and $a^T a = \|a\|^2$, we can simplify (34) to obtain

$$\begin{aligned} \dot{V} \leq & \|Y_1(\cdot)\| \|\tilde{\Phi}_1\| \|r\| - K_{v_m} \|r\|^2 - \frac{\rho_1^2 \|r\|^2}{\rho_1 \|r\| + \varepsilon^2} + \\ & \|Y_2(\cdot)\| \|\tilde{\Phi}_2\| \|\eta\| + \|L_m\| \|\dot{I}_d\| \|\eta\| - \\ & \frac{\rho_2^2 \|\eta\|^2}{\rho_2 \|\eta\| + \mu^2} - \varepsilon^2 - \mu^2. \end{aligned} \tag{35}$$

Consider two bounded sets such as $\Omega_1 = \{E(t) \mid \|E(t)\| \leq \ell\}$, $\Omega_2 = \{E(0) \mid \|E(0)\| \leq \sqrt{\frac{P_m}{P_M}} \ell\}$ where ℓ is a selected positive scalar which defines the boundary of the sets. For any trajectory in Ω_1 , since e and \dot{e} are bounded (21) results in bounded \ddot{e} , too. Utilizing (16), (19) and (27) in (35), for any trajectory in Ω_1 it can

be stated that

$$\begin{aligned} \dot{V} \leq & -K_{v_m} \|r\|^2 + \rho_1 \|r\| - \frac{\rho_1^2 \|r\|^2}{\rho_1 \|r\| + \varepsilon^2} + \\ & \rho_2 \|\eta\| - \frac{\rho_2^2 \|\eta\|^2}{\rho_2 \|\eta\| + \mu^2} - \varepsilon^2 - \mu^2 \leq \\ & -K_{v_m} \|r\|^2 - \frac{\varepsilon^4}{\rho_1 \|r\| + \varepsilon^2} - \frac{\mu^4}{\rho_2 \|\eta\| + \mu^2} \end{aligned} \tag{36}$$

and consequently

$$\dot{V} \leq -K_{v_m} \|r\|^2. \tag{37}$$

Since Ω_2 is a subset of Ω_1 , for any trajectory initialized in Ω_2 one can integrate (37) to obtain

$$V(t) - V(0) \leq -K_{v_m} \int_0^t \|r\|^2 dt. \tag{38}$$

Using (7) in the above equation, we can write

$$\begin{aligned} \frac{1}{2} P_m \|E(t)\|^2 \leq & V(t) \leq V(0) - K_{v_m} \int_0^t \|r\|^2 dt \leq \\ \frac{1}{2} P_M \|E(0)\|^2 - & K_{v_m} \int_0^t \|r\|^2 dt \end{aligned} \tag{39}$$

or

$$\|E(t)\| \leq \sqrt{\frac{P_M}{P_m}} \|E(0)\| \leq \ell. \tag{40}$$

Therefore, from the definition of Ω_2 for any trajectory initialized in Ω_2 , it can be stated that

$$\|E(t)\| \leq \ell, \quad \forall t > 0 \tag{41}$$

which concludes that any trajectory starting in Ω_2 will remain in Ω_1 .

Also from (39) we can conclude that

$$\lim_{t \rightarrow \infty} \|E(t)\|^2 \leq \frac{P_M}{P_m} \|E(0)\|^2 - \frac{K_{v_m}}{P_m} \int_0^\infty \|r\|^2 dt. \tag{42}$$

Hence it can be stated that

$$\lim_{t \rightarrow \infty} \|r\| = 0. \tag{43}$$

Note that (10) is a stable first-order differential equation driven by the input r . Therefore, by standard linear control arguments and (10), we can state

$$\lim_{t \rightarrow \infty} e = 0 \quad \text{and} \quad \lim_{t \rightarrow \infty} \dot{e} = 0. \tag{44}$$

The above results state that the tracking errors e and \dot{e} are asymptotically stable. \square

5 Applications to robotic systems interacting with environment

In Section 3, a robust controller is designed for unconstrained serial manipulators. In many industrial/manufacturing applications such as welding, forming, assembling, and grinding, a robot manipulator is required to come into a planned contact with the environment. In these

applications, the environment somehow imposes some constraints on the trajectories that the robot must follow. In this section, the proposed control method will be extended to the case of nonredundant constrained robotic systems.

5.1 Constrained robot dynamics

Dynamic motion of constrained robotic systems interacting with rigid environment is described by [27]:

$$M'(q)\ddot{q} + C'(q, \dot{q})\dot{q} + g'(q) + J_e^T f_n + J_f^T \tau_d + f'(\dot{q}) = \tau \tag{45}$$

where $q, M', C', g', \tau_d, J_f', f', \tau$ have the same definitions as serial robot manipulators. $f_n \in \mathbf{R}^n$ denotes the end-effector normal forces of contact described in the task space and $J_e \in \mathbf{R}^{n \times n}$ represents the Jacobian matrix of the system.

Here we assume that the manipulator operates away from any singularity and that the manipulator motion is holonomically constrained by m algebraic equations. These constraints in the velocity space are expressed by

$$D \dot{X} = D J_e(q) \dot{q} = 0 \tag{46}$$

where \dot{X} represents the task space velocity of the end effector and $D \in \mathbf{R}^{m \times n}$ is a full row rank matrix.

The normal contact force can be represented by

$$f_n = D^T \lambda \tag{47}$$

where λ denotes the generalized Lagrangian multiplier.

Consider the matrix D_e denoted by

$$D_e = D(q) J_e(q). \tag{48}$$

As mentioned in [27], without loss of generality one can partition the columns of the matrix D_e as

$$D_e = [D_{ml} | D_m] \tag{49}$$

where $D_m \in \mathbf{R}^{m \times m}$ is an m squared nonsingular matrix and $D_{ml} \in \mathbf{R}^{m \times l}$, $l = n - m$.

Due to m holonomic constraints, the joint space of the robot has only l independent variables and one can always partition the joint position vector to $q_l \in \mathbf{R}^l$ and $q_m \in \mathbf{R}^m$ as

$$q = \begin{bmatrix} q_l \\ q_m \end{bmatrix}. \tag{50}$$

Due to m holonomic constraints, it can be mentioned that $q = \Omega(q_l)$ where Ω is a nonlinear mapping function which is bounded for bounded state variable q_l . It then follows that

$$\dot{q} = J_l(q) \dot{q}_l \tag{51}$$

where

$$J_l(q) = \begin{bmatrix} I_l \\ -D_m^{-1} D_{ml} \end{bmatrix} \tag{52}$$

and $I_l \in \mathbf{R}^{l \times l}$ is an identity matrix. It is not difficult to see that

$$J_l^T D_e^T = 0. \tag{53}$$

Equation (53) is very useful in the controller design and stability analysis of the system.

By the following change of variables, one can decouple the robot dynamic into two individual blocks: a reduced position block and a reduced force block. It is worth to mention that the constrained force does not appear in the reduced position model. Considering (4), (51) and (53), the reduced position block can be represented by

$$M_l(q)\ddot{q}_l + C_l(q, \dot{q}_l)\dot{q}_l + G_l(q) + J_l^T (J_f^T \tau_d + f(\dot{q})) = I_l \tag{54}$$

where

$$\begin{aligned} M_l(q) &= K_{Tm}^{-1} J_l^T M'(q) J_l \\ C_l(q, \dot{q}_l) &= K_{Tm}^{-1} J_l^T \left(M'(q) \dot{J}_l + C'(q, \dot{q}_l) \right) \\ G_l(q) &= K_{Tm}^{-1} J_l^T g'(q) \\ J_f &= J_f' K_{Tm}^{-T}, \quad f(\dot{q}) = K_{Tm}^{-1} f'(\dot{q}) \\ I_l &= J_l^T I. \end{aligned} \tag{55}$$

The brushed DC (BDC) motors dynamics can be modeled as

$$L_m \dot{I}_l = L_m J_l^T I - J_l^T R_m I - J_l^T K_{em} \dot{q} + v_l \tag{56}$$

where $v_l = J_l^T v$, I and v represent the motor current and motor voltage, respectively. And L_m, R_m, K_{em} represent the actuators inductance matrix, the actuators resistance matrix and the motors back emf coefficient matrix, respectively.

It is worth to mention that the matrix $M_l(q)$ is positive definite, and that the matrix $\frac{1}{2} \dot{M}_l(q) - C_l(q, \dot{q}_l)$ is skew symmetric.

5.2 Controller design

Let us define the filtered tracking error by

$$r_l = \dot{e}_l + \Lambda e_l \tag{57}$$

where $\dot{e}_l = \dot{q}_l - \dot{q}_{ld}$, $e_l = q_l - q_{ld}$ and q_{ld}, \dot{q}_{ld} are the desired values of reduced position and velocity vectors, respectively.

Also, let us define

$$\begin{aligned} Y_{l1}(q, \dot{q}, t) \Phi_{l1} &= M_l (\Lambda \dot{e}_l - \ddot{q}_{ld}) - g_l(q) - \\ &C_l(q, \dot{q}) (-\Lambda e_l + \dot{q}_{ld}) - J_l^T (J_f^T \tau_d + f(\dot{q})) \\ Y_{l2}(q, \dot{q}, I, t) \Phi_{l2} &= L_m J_L^T I - J_L^T (R_m I + K_{em} \dot{q}) \end{aligned} \tag{58}$$

where $Y_{l1}(\cdot)$ is the mechanical regressor matrix, $Y_{l2}(\cdot)$ is the electrical regressor matrix, Φ_{l1} represents uncertain mechanical parameters and Φ_{l2} represents uncertain electrical parameters.

Consider the current tracking error defined by

$$\eta_l = I_l - I_{ld} \tag{59}$$

where I_{ld} represents the desired current trajectory calculated by

$$I_{ld} = -K_v r_l - Y_{l1}(\cdot) \bar{\Phi}_{l1} - \frac{\rho_{l1}^2 r_l}{\rho_{l1} \|r_l\| + \varepsilon^2} \quad (60)$$

where

$$\rho_{l1} = \alpha_{l1} \|Y_{l1}(\cdot)\| \quad (61)$$

$$\dot{\varepsilon} = -K_\varepsilon \varepsilon. \quad (62)$$

$\bar{\Phi}_{l1}$ represents the nominal values of the uncertain mechanical parameters and we can assume that $\|\tilde{\Phi}_{l1}\| \leq \alpha_{l1}$, where $\tilde{\Phi}_{l1} = \Phi_{l1} - \bar{\Phi}_{l1}$ and no restriction exists on the magnitude of α_{l1} . Let us introduce the control law for the motor voltage as

$$v_l = -Y_{l2}(\cdot) \bar{\Phi}_{l2} - r_l - \frac{\rho_{l2}^2 \eta_l}{\rho_{l2} \|\eta_l\| + \mu^2} \quad (63)$$

where

$$\rho_{l2} = \alpha_{l2} \|Y_{l2}(\cdot)\| + l\alpha_{l3} \quad (64)$$

$$\dot{\mu} = -K_\mu \mu. \quad (65)$$

Similar to Φ_{l1} , it can be assumed that $\|\tilde{\Phi}_{l2}\| \leq \alpha_{l2}$ where $\tilde{\Phi}_{l2} = \Phi_{l2} - \bar{\Phi}_{l2}$ and no restriction exists on the magnitude of α_{l2} . α_{l3} is defined similar to α_3 , i.e., $\|\dot{I}_{ld}\| \leq \alpha_{l3}$.

Consequently, the position and current error dynamics can be represented by

$$M_l \dot{r}_l = Y_{l1}(\cdot) \tilde{\Phi}_{l1} - C_l(q, \dot{q}_l) r_l - K_v r - \frac{\rho_{l1}^2 r_l}{\rho_{l1} \|r_l\| + \varepsilon^2} + \eta_l \quad (66)$$

$$L_m \dot{\eta}_l = -L_m \dot{I}_{ld} + Y_{l2}(\cdot) \tilde{\Phi}_{l2} - \frac{\rho_{l2}^2 \eta_l}{\rho_{l2} \|\eta_l\| + \mu^2} - r_l.$$

The stability and performance of the whole control system in trajectory tracking is analyzed by Theorem 2.

Theorem 2. The input control voltage calculated by (63), results in semi-global asymptotic stability of position and velocity tracking error, i.e.,

$$\lim_{t \rightarrow \infty} e_l = 0, \quad \lim_{t \rightarrow \infty} \dot{e}_l = 0 \quad (67)$$

provided that the desired trajectory tracking and the initial system errors being bounded.

The stability of the system can be proved by the same procedure presented in Section 4, utilizing the following Lyapunov function:

$$V(E_l) = \frac{1}{2} E_l^T P E_l \quad (68)$$

where $E_l = [r_l^T, \eta_l^T, \varepsilon, \mu]^T$ is the augmented state vector and

$$P = \text{diag} \{ M_l, L_m, K_\varepsilon^{-1}, K_\mu^{-1} \}. \quad (69)$$

6 Experimental and numerical implementation

In order to validate the proposed method, in this section experimental and numerical results are presented for two different systems: A two link serial manipulator and a four-bar linkage system.

6.1 Experimental setup

The developed controller is implemented experimentally on a two link planar manipulator shown in Fig. 1 and the experimental results are compared with those of the simulation results for the same system parameters. Each axis is driven by a Maxon servomotor set consisting of a BDC, an encoder and a gear reduction unit. The mass and the length of the links, without considering the mass of the motors, are approximately about 0.54 kg and 43 cm for the first link and 0.24 kg and 47 cm for the second one. The mass of the first and the second motors sets are 0.45 kg and 0.32 kg, respectively.



Fig.1 The two link planar manipulator employed for experimental results

The base and elbow joints have the capability of making up to 0.85 and 1.6 revolutions per second and each one has maximum position feedback resolution of up to 14400 counts per revolution. The base motor is capable of generating up to 16.7 N-m torque and the elbow motor up to 2.2 N-m. The effective torque constant at the joint ends are 6.1 N-m/A for the first axis and 1.95 N-m/A for the second one.

Real-time control is performed with a host computer (Pentium IV 2.0 GHz dual-core) and a servo 400 MHz DSP. Each motor is mounted on two ball bearings after gearbox. The gearboxes have planar clearance of approximately up to 1 deg. This leads to a resultant clearance of 1.5 cm at the end-effector point. For the velocity feedback, a one step numerical differentiation of the joint position measurements with a sampling period of 4 ms has been used.

6.2 Experimental and numerical results for a two link manipulator

Using the above mentioned numerical values of system parameters and employing the proposed algorithm, the controller is developed. The following are used as the control

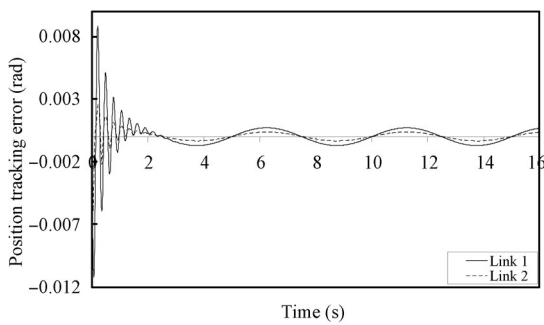
gains:

$$\begin{aligned} K_v &= \text{diag} \{100, 100\} \\ K_\epsilon &= K_\mu = 0.001 \\ \epsilon(0) &= \mu(0) = 100 \\ \Lambda &= \text{diag} \{10, 10\}. \end{aligned} \tag{70}$$

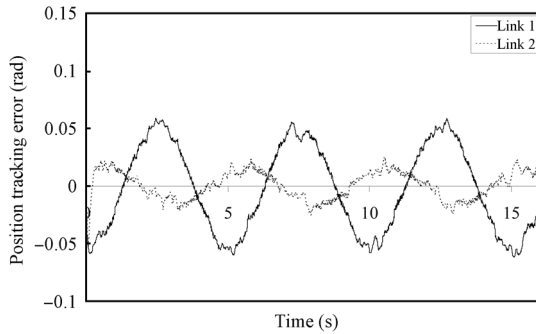
The robot is assumed to track a harmonic desired trajectory defined by (71), while the electrical and mechanical parameters are in fact uncertain.

$$q_{1d} = q_{2d} = 0.5 \sin \frac{2\pi}{5} t. \tag{71}$$

The position and velocity tracking errors, both for the experimental results and numerical simulation are given in Figs. 2 and 3.



(a) Simulation results

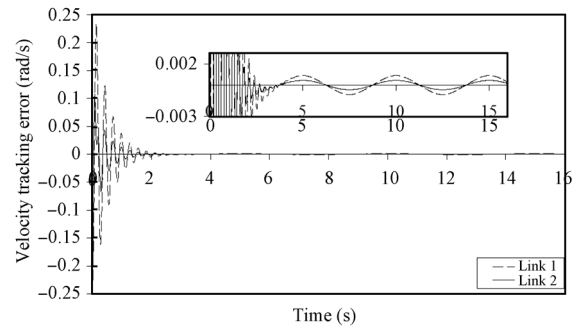


(b) Experimental results

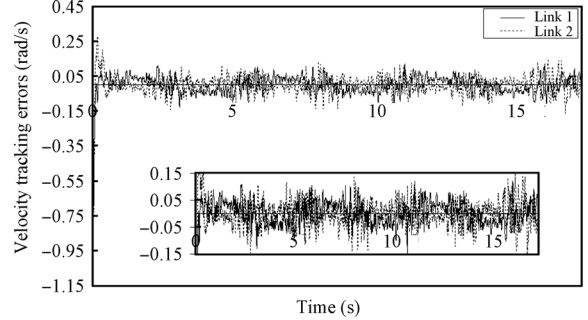
Fig. 2 Time history of position tracking errors

Fig. 2 shows that the absolute maximum position tracking error for joint 1 is about 0.06 rad (3.43 deg) and it is about 0.02 rad (1.14 deg) for joint 2 in the experimental case, once the initial errors get settled down. These values are 0.003 rad (0.17 deg) for link 1 and 0.001 rad (0.05 deg) for link 2 in the simulation results, once the initial errors get settled down.

The velocity tracking errors are given in Fig. 3. There is an initial spike in the velocity tracking error at $t = 0$. This can be seen again in experimental and simulation results. It is due to the initial condition errors. This figure shows that in the experimental case the velocity tracking errors are bounded within 0.15 rad/s for both links, once the initial errors get settled down. However, in the simulation case they are bounded to 0.006 rad/s and 0.003 rad/s, respectively.



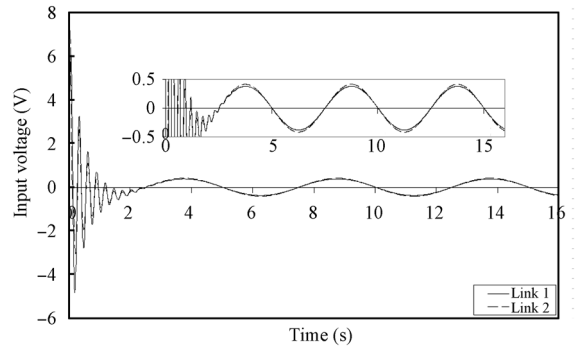
(a) Simulation results



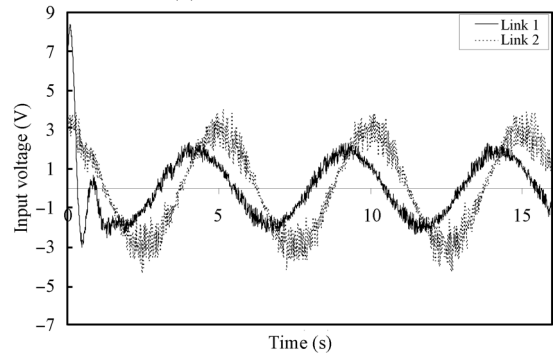
(b) Experimental results

Fig. 3 Time history of velocity tracking errors

Fig. 4 shows time history of the motors input voltage. Except for noisy behavior of the experimental results, similarity and closeness of the experimental results and simulation results can be clearly observed.



(a) Simulation results



(b) Experimental results

Fig. 4 Time history of input voltage

6.3 Numerical results for a four-bar linkage system

In this section, the validity of the theorem presented in Section 5 is verified by the numerical simulation executed on a four-bar linkage, as an example of constrained robotic systems. The schematic of the system is shown in Fig. 5 which is driven by a motor installed on the first link.

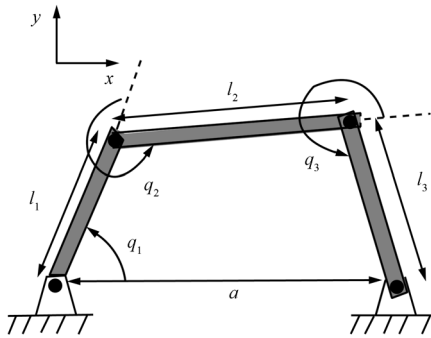


Fig. 5 Schematic of a four-bar linkage

The dynamics of the system is calculated by (54) and (56), and the inertia and Coriolis and gravity terms are calculated for a three link robotic arm utilizing the Maple software.

A four-bar linkage has two constraint equations defined by

$$\begin{aligned} l_1 c_1 + l_2 c_{12} + l_3 c_{123} &= a \\ l_1 s_1 + l_2 s_{12} + l_3 s_{123} &= 0. \end{aligned} \tag{72}$$

Also $D(q)$ and $J_e(q)$ are defined by

$$D = \begin{bmatrix} 1 & 0 \\ 0 & 1 \end{bmatrix}, \quad J_e = \begin{bmatrix} -l_1 s_1 & -l_2 s_{12} & -l_3 s_{123} \\ l_1 c_1 & l_2 c_{12} & l_3 c_{123} \end{bmatrix}. \tag{73}$$

Considering $q_l = q_1$ and $q_m = [q_2, q_3]^T$ and utilizing the Maple software, the reduced order dynamics of the system in the form of (45) is computed. The electromechanical parameters of the system are selected by

$$\begin{aligned} m_1 &= 1 \text{ kg}, m_2 = 1 \text{ kg}, m_3 = 1 \text{ kg}, \\ l_1 &= 1 \text{ m}, l_2 = 1 \text{ m}, l_3 = 1 \text{ m}, a = 2 \text{ m}, \\ K_T &= 1, L_m = 0.1 \text{ H}, K_{em} = 0.2 \text{ V} \cdot \text{s/rad}, R_m = 5 \Omega. \end{aligned} \tag{74}$$

The uncertain mechanical parameter vector is $\Phi_1 = [m_1, m_2, m_3]^T$ and the uncertain electrical parameter vector is $\Phi_2 = [L_m, K_{em}, R_m]^T$. The desired trajectory for q_1 is described by

$$q_{1d} = \sin t. \tag{75}$$

The nominal values of the uncertain parameters are assumed to be $\bar{\Phi}_1 = [6, 6, 6]^T$, $\bar{\Phi}_2 = [2, 2, 8]^T$. The nominal magnitude of parameters are selected far from their actual

values to show the effectiveness of the method against great degrees of uncertainties.

Here, for the convenience of simulation, the entire initial conditions are assumed to be zero and the controller gains for the proposed method are chosen to be

$$\begin{aligned} K_v &= 100, \Lambda = 3 \\ K_\epsilon &= K_\mu = 0.001 \\ \epsilon(0) &= \mu(0) = 100. \end{aligned} \tag{76}$$

The simulation results are presented in Figs. 6–8. The angular position tracking error, e_l , is represented in Fig. 6. The angular velocity tracking error, \dot{e}_l , is shown in Fig. 7. The motor voltage is plotted in Fig. 8.

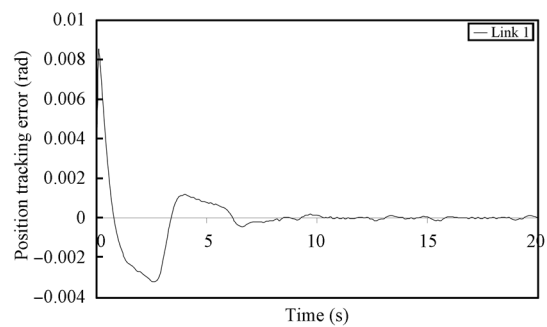


Fig. 6 Time history of position tracking error

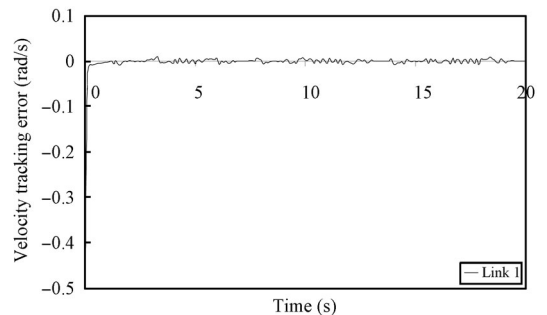


Fig. 7 Time history of velocity tracking error

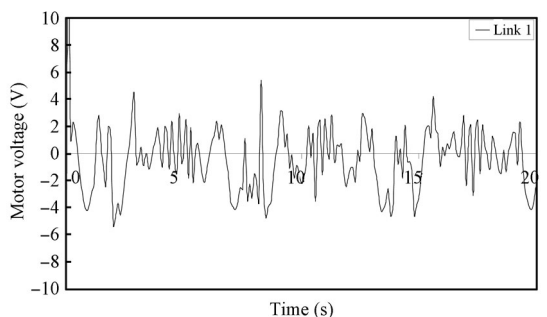


Fig. 8 Time history of input voltage

From this comparative simulation, it can be concluded that the joint position and velocity of the robot system converge towards the desired trajectories.

7 Conclusions

In this paper, a robust control law has been presented to ensure trajectory tracking for electrically driven robotic systems considering both the robot and actuators uncertainties. In the presented method, no statistical information about the uncertain elements is assumed. The proposed robust control law has two advantages over the previous ones. First, the proposed control law results in asymptotic stability while the majority of the robust methods guarantee the boundedness of the tracking error. The second advantage comes from considering both robot and actuators uncertainties. The method is employed to control two different case studies; a two link serial manipulator and a four-bar linkage system. Both numerical and experimental results show the effectiveness of the method in controlling the system.

References

- [1] Z. H. Qu, D. M. Dawson. *Robust Tracking Control of Robot Manipulators*, Piscataway, USA: IEEE Press, 1996.
- [2] C. Abdallah, D. Dawson, P. Dorato, M. Jamshidi. Survey of robust control for rigid robots. *IEEE Control Systems*, vol. 11, no. 2, pp. 24–30, 1991.
- [3] J. H. Shin, K. B. Park, S. W. Kim, J. J. Lee. Robust adaptive control for robot manipulators using regressor-based form. In *Proceedings of IEEE International Conference on Systems Manufacturing and Cybernetics*, IEEE, San Antonio, USA, vol. 3, pp. 2063–2068, 1994.
- [4] J. Huang, Z. Chen. A general framework for tackling the output regulation problem. *IEEE Transactions on Automatic Control*, vol. 49, no. 12, pp. 2203–2218, 2004.
- [5] M. Boukattaya, T. Damak, M. Jallouli. Robust adaptive control for mobile manipulators. *International Journal of Automation and Computing*, vol. 8, no. 1, pp. 8–13, 2011.
- [6] M. Z. Hou, A. G. Wu, G. R. Duan. Robust output feedback control for a class of nonlinear systems with input unmodeled dynamics. *International Journal of Automation and Computing*, vol. 5, no. 3, pp. 307–312, 2008.
- [7] M. W. Spong. On the robust control of robot manipulators. *IEEE Transactions on Automatic Control*, vol. 37, no. 11, pp. 1782–1786, 1992.
- [8] G. Liu. Decomposition-based control of mechanical systems. In *Proceedings of the Canadian Conference on Electrical and Computer Engineering*, IEEE, Halifax, Canada, vol. 2, pp. 966–970, 2000.
- [9] H. D. Taghirad, M. A. Khosravi. Design and simulation of robust composite controllers for flexible joint robots. In *Proceedings of ICRA IEEE International Conference on Robotics and Automation*, IEEE, Taipei, Taiwan, China, vol. 3, pp. 3108–3113, 2003.
- [10] C. Ham, Z. Qu, R. Johnson. Robust fuzzy control for robot manipulators. In *Proceedings of Control Theory Applications*, vol. 147, no. 2, pp. 212–216, 2000.
- [11] Q. J. Chen, H. T. Chen, Y. J. Wang, P. Y. Woo. Robust adaptive trajectory tracking independent of models for robotic manipulators. *Journal of Robotic Systems*, vol. 18, no. 9, pp. 545–551, 2001.
- [12] D. K. Chwa. Sliding-mode tracking control of nonholonomic wheeled mobile robots in polar coordinates. *IEEE Transactions on Control System Technology*, vol. 12, no. 4, pp. 637–644, 2004.
- [13] Z. P. Wang, S. S. Ge, T. H. Lee. Robust motion/force control of uncertain holonomic/nonholonomic mechanical systems. *IEEE Transactions on Mechatronics*, vol. 9, no. 1, pp. 118–123, 2004.
- [14] B. Bandyopadhyay, S. Janardhanan, V. Sreeram. Sliding mode control design via reduced order model approach. *International Journal of Automation and Computing*, vol. 4, no. 4, pp. 329–334, 2007.
- [15] M. M. Fateh, S. Fateh. A precise robust fuzzy control of robots using voltage control strategy. *International Journal of Automation and Computing*, vol. 10, no. 1, pp. 64–72, 2013.
- [16] M. Homayounzade, M. Keshmiri. On the robust tracking control of kinematically constrained robot manipulators. In *Proceedings of IEEE International Conference on Mechatronics*, IEEE, Istanbul, Turkey, pp. 248–253, 2011.
- [17] M. C. Good, L. M. Sweet, K. L. Strobel. Dynamic models for control system design of integrated robot and drive systems. *Journal of Dynamic System Measurement and Control*, vol. 107, no. 1, pp. 53–59, 1985.
- [18] T. J. Tarn, A. K. Bejczy, X. Yun, Z. Li. Effect of motor dynamics on nonlinear feedback robot arm control. *IEEE Transactions on Robotics and Automation*, vol. 7, no. 1, pp. 114–122, 1991.
- [19] D. M. Dawson, Z. Qu, J. J. Carol. Tracking control of rigid-link electrically driven robot manipulator. *International Journal of Control*, vol. 56, no. 5, pp. 911–1006, 1992.
- [20] C. Ishii, T. Shen, Z. Qu. Lyapunov recursive design of robust tracking control with L_2 -gain performance for electrically-driven robot manipulators. *International Journal of Control*, vol. 74, no. 8, pp. 811–828, 2001.
- [21] J. P. Hwang, E. Kim. Robust tracking control of an electrically driven robot: Adaptive fuzzy logic approach. *IEEE Transactions on Fuzzy Systems*, vol. 14, no. 2, pp. 232–247, 2006.
- [22] Y. C. Chang, T. Hsien. Adaptive tracking control for electrically-driven robots without overparameterization. *International Journal of Adaptive Control and Signal Processing*, vol. 16, no. 2, pp. 123–150, 2002.
- [23] M. M. Fateh, M. Baluchzadeh. Modeling and robust discrete LQ repetitive control of electrically driven robots. *International Journal of Automation and Computing*, vol. 10, no. 5, pp. 472–480, 2013.
- [24] M. M. Fateh. Robust control of electrical manipulators by joint acceleration. *International Journal of Innovative Computing, Information and Control*, vol. 6, no. 12, pp. 5501–5510, 2010.

- [25] M. M. Fateh, H. A. Tehrani, S. M. Karbassi. Repetitive control of electrically driven robot manipulators. *International Journal of Systems Science*, vol. 44, no. 4, pp. 775–785, 2011.
- [26] J. Slotine, W. Li. Theoretical issues in adaptive control. In *Proceedings of the 5th Yale Workshop on Applications of Adaptive Systems Theory*, New Haven, USA, pp. 252–259, 1985.
- [27] K. Khayati, P. Bigras, L. A. Dessaint. A multistage position/force control for constrained robotic systems with friction: Joint-space decomposition, linearization, and multi-objective observer/controller synthesis using LMI formalism. *IEEE Transactions on Industrial Electronics*, vol. 53, no. 5, pp. 1698–1712, 2006.



Mohamadreza Homayounzade received his B.Sc. and M.Sc. degrees in mechanical engineering from Shiraz University and Isfahan University of Technology (IUT), Iran in 2008 and 2010, respectively. He is currently pursuing his Ph.D. degree in the Department of Mechanical Engineering in robotics and control) in IUT, Isfahan, Iran.

His research interests include the application of nonlinear control techniques to mechanical and electromechanical systems.

E-mail: m.homayounzade@me.iut.ac.ir (Corresponding author)

ORCID iD: 0000-0002-8477-1501



Mehdi Keshmiri received his B.Sc. and M.Sc. degrees in mechanical engineering from Sharif University of Technology, Tehran, Iran in 1986 and 1989, respectively. He received his Ph.D. degree in mechanical engineering (space dynamics) from McGill University, Montreal, Canada. He is currently an associate professor in the Department of Mechanical Engineering of Isfahan

University of Technology (IUT), Isfahan, Iran. He joined IUT as soon as he finished his Ph.D. in 1995. He has presented and published more than 100 papers in international conferences and journals and supervised more than 60 Ph.D. and master students.

His research interests include system dynamics, control systems and dynamics and control of robotic systems.

E-mail: mehdik@cc.iut.ac.ir



Mostafa Ghobadi received his B.Sc. and M.Sc. degrees in mechanical engineering from Isfahan University of Technology (IUT), Isfahan, Iran. He is currently pursuing his Ph.D. degree in the Department of Mechanical Engineering at University at Buffalo SUNY, New York, USA.

His research interests include human motion analysis and theory, human activity recognition, smart human-machine interface, filtering and estimation theory, robot's dynamics and control, and bipedal locomotion.

E-mail: m.ghobadishahreza@me.iut.ac.ir